

DynamiCtrl: Rethinking the Basic Structure and the Role of Text for High-quality Human Image Animation

Haoyu Zhao¹ Zhongang Qi² Cong Wang³ Qingping Zheng⁴ Guansong Lu²
Fei Chen² Hang Xu² Zuxuan Wu¹

¹ Fudan University, China ² Huawei Noah’s Ark Lab, China

³ Sun Yat-sen University, China ⁴ Zhejiang University, China

¹{hyzhao22@m., zxwu}@fudan.edu.cn

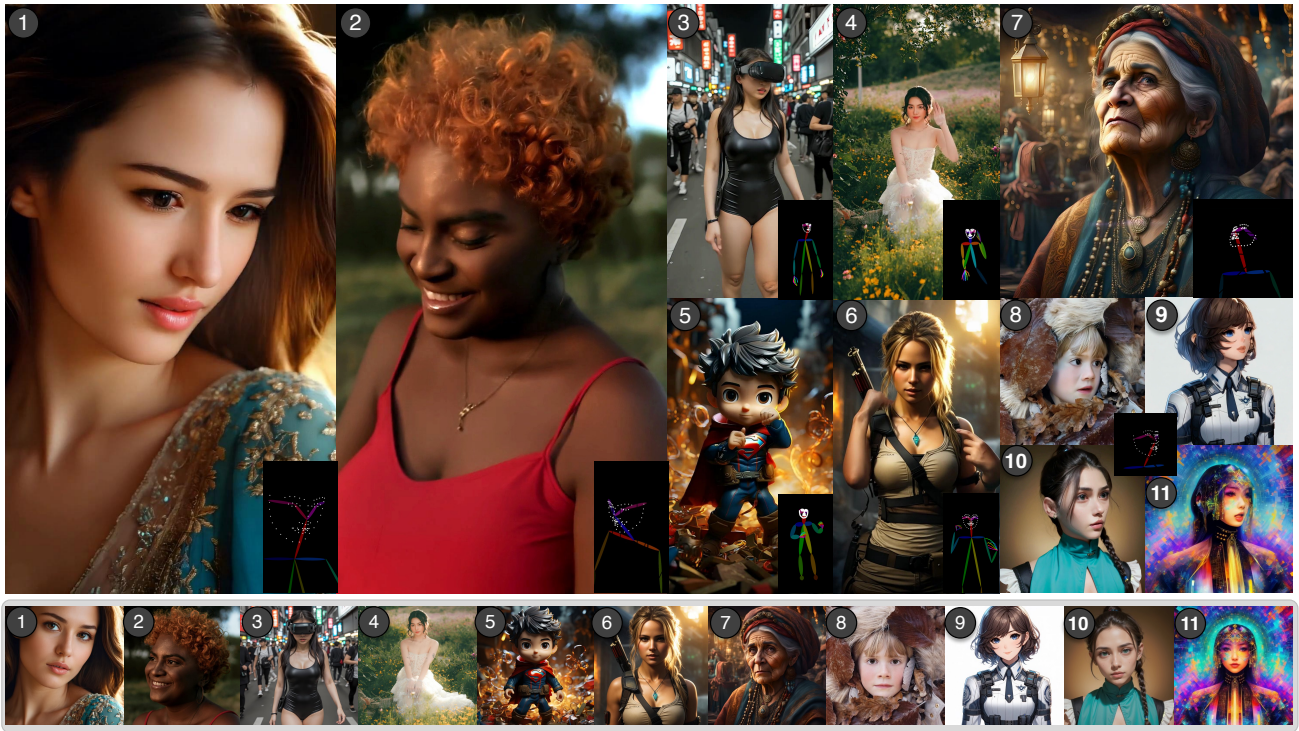


Figure 1. DynamiCtrl with image, pose, and text control in transformer backbone achieves state-of-the-art human video generation quality. We show generated frames in the top line, with these examples being generated by driving the bottom humans in different pose videos.

Abstract

Human image animation has recently gained significant attention due to advancements in generative models. However, existing methods still face two major challenges: (1) architectural limitations—most models rely on U-Net, which underperforms compared to the MM-DiT; and (2) the neglect of textual information, which can enhance controllability. In this work, we introduce DynamiCtrl, a novel framework that not only explores different pose-guided control structures in MM-DiT but also reemphasizes the crucial

role of text in this task. Specifically, we employ a Shared VAE encoder for both reference images and driving pose videos, eliminating the need for an additional pose encoder and simplifying the overall framework. To incorporate pose features into the full attention blocks, we propose Pose-adaptive Layer Norm (PadaLN), which utilizes adaptive layer normalization to encode sparse pose features. The encoded features are directly added to the visual input, preserving the spatiotemporal consistency of the backbone while effectively introducing pose control into MM-DiT. Furthermore, within the full attention mechanism, we align

Methods	Max resolution	LPIPS metric ↓	Image control	Pose control	Text control	Background synthesis	W/O extra Pose-encoder
AnimateAnyone [11]	784 × 512	0.285	✓	✓	✗	✗	✗
Champ [44]	512 × 512	0.231	✓	✓	✗	✗	✗
MimicMotion [40]	1024 × 576	0.414	✓	✓	✗	✗	✗
StableAnimator [24]	1024 × 576	0.232	✓	✓	✗	✗	✗
Animate-X [23]	768 × 512	0.232	✓	✓	✗	✗	✗
DynamiCtrl	1360 × 1360	0.166	✓	✓	✓	✓	✓

Table 1. A system-level comparison between DynamiCtrl and existing State-of-the-Art human image animation frameworks.

textual and visual features to enhance controllability. By leveraging text, we not only enable fine-grained control over the generated content, but also, for the first time, achieve simultaneous control over both background and motion. Experimental results verify the superiority of DynamiCtrl on benchmark datasets, demonstrating its strong identity preservation, heterogeneous character driving, background controllability, and high-quality synthesis. The project page is available at github.com/gulucaptain/DynamiCtrl.

1. Introduction

With the rapid and magical growth the AIGC field is experiencing, human image animation, as a task specifically for human motion video generation, has also gained increasing attention [3, 13, 15, 20, 22, 35]. The task aims to generate videos based on a guided pose sequence and a reference human image, which is applied in social media, animation production, and digital human domains. Previous works [11, 26, 28, 32, 40, 44] have achieved promising results in this task by utilizing U-Net-based generative models [2, 4, 8, 43] as the backbone.

Recently, represented by Sora, the MM-DiT architecture has been widely used [7, 18, 37] and demonstrates superior quality in generating image and video content. This also sparked exploration into how conditional controls can be implemented within MM-DiT. In image generation, method [18] uses the adaptive layer normalization to encode label categories, thereby controlling image generation. From Gentron [5] and Hunyuan-DiT [14], we find cross-attention is more effective than layer norm when control the textual prompt. In video generation, CogVideoX [37] and EasyAnimate [33] adopt the in-context function, which directly concatenate the image condition with input noise. Currently, few works have attempted to introduce pose control signals into the MM-DiT architecture, especially for human image animation tasks that involve multiple inputs. Therefore, it is necessary to explore pose control within MM-DiT and develop a new basic structure for this task.

Besides, the widely used control signal, the textual prompt, is ignored in most previous works on this task. For instance, in the early work Animate Anyone [11] and Moore [16], the textual features are directly replaced with

image features generated by ReferenceNet. Later, in MimicMotion [40], the overall approach is implemented using the Stable Video Diffusion model [2], which does not include textual control conditions. So, we raise the question: *Is textual information truly unhelpful for this task?* We observe that text can control the details of images and videos through text prompts, including subject appearance, actions, and qualities. We believe that text information can provide fine-grained semantic features aligned with reference images, helping the model understand complex human clothing, makeup, and diverse characters, including real individuals, cartoon figures, and artistic styles.

In this work, we propose a novel framework for human image animation, named DynamiCtrl, which can generate human videos with high quality, ID fidelity, and controllability (shown in Fig. 1). In our model, we explore three different structures to control the pose signal in MM-DiT and reconsider the role of text in this task. Specifically, to effectively encode the pose sequence, instead of training an additional pose encoder as in previous works [11, 24, 28, 40, 44], we use Shared VAE encoder for images to encode the pose sequence, ensuring the simplicity of our framework. Then, we propose the Pose-adaptive Layer Norm (PadaLN) to introduce the pose feature into the MM-DiT blocks. We find that using cross-attention for pose injection not only brings a huge amount of additional parameters, but also leads to inaccurate pose control. Similarly, the in-context method also causes instability in temporal sequences and visual forgetting. Differently, our proposed PadaLN encodes pose features by applying adaptive layer normalization individually and directly adds them to the visual tokens. As a result, we can effectively introduce pose signals into the MM-DiT to achieve motion control.

Moreover, in DynamiCtrl, we reconsider the role of text in the human image animation task. We employ three conditions to control video generation, *i.e.*, reference images, driving poses, and textual prompts. In MM-DiT blocks, the text tokens and visual tokens interact through full attention. We observe that textual prompts can effectively enable fine-grained improvements while ensuring accurate pose control. For example, we can add prompts to fix the defects or control the expressions at the same time. Furthermore, by using the masks for the reference individuals, we can precisely control the video background, significantly

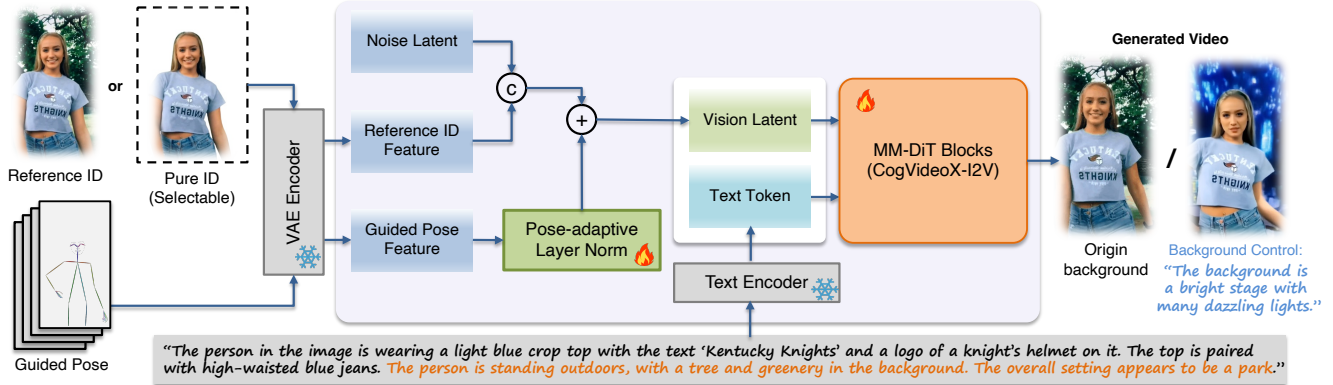


Figure 2. Overview of the proposed DynamiCtrl for human image animation. We primarily explore how to achieve pose control within the MM-DiT structure and emphasize the important role of text in this task. We also demonstrate the background controllability by only replacing the background description in orange with the one in blue, *i.e.*, “tree and greenery” to “dazzling lights”.

enhance the model’s generation ability, and create more diverse videos. In Table 1, We conduct a system-level comparison between our model and existing methods. In experiments, we validate the effectiveness of DynamiCtrl on the public and self-built Unseen datasets. The results demonstrate that our model achieves new state-of-the-art or at least competitive results in both the quantitative and qualitative aspects, *e.g.*, best LPIPS result of 0.166.

In short, our work makes the following contributions:

- We propose a novel DynamiCtrl framework for human image animation, which is based on the MM-DiT architecture. We explore different pose control structures and propose the Pose-adaptive Layer Norm to achieve better alignment between the driving poses and the videos.
- We refocus on the role of textual prompts in human image animation. We align features between text and visual inputs to achieve fine-grained controllability, including background control while maintaining pose accuracy. To our knowledge, we are the first to introduce text into this task and successfully achieve background control.
- Experimental results on benchmark datasets demonstrate that our DynamiCtrl surpasses competing methods both quantitatively and qualitatively. Moreover, our approach is capable of generating high-quality, controllable videos at resolutions of up to 1360×1360 , ensuring fine-grained details and enhanced identity fidelity.

2. Related work

Image and Video Generation. Diffusion Models [2, 8, 9, 18, 37, 42, 43] have recently demonstrated impressive results in image and video synthesis. Earlier, U-Net-based models demonstrated satisfactory performance in text control and visual expression. Image diffusion models [21] aim to learn to generate high-quality images through a process of progressive denoising, while video diffusion models [2] focus on achieving good temporal consistency. Meth-

ods [4, 17, 29, 43] rely on temporal layers or 3D structure to keep temporal consistency. Later, with the rise of the Sora, models based on the DiT architecture gradually became mainstream, showing stronger performance in terms of generation quality, including both image [14, 18] and video [33, 37] generation.

Human Image Animation. Human image animation refers to the process of creating a dynamic video that depicts human motion based on pose sequences, typically generated by diffusion models. In the early stage, image-diffusion-based methods [11, 13, 15, 20, 22, 26, 28, 32] typically rely on post-processing to generate human motion video, which often leads to loss of detail and heavy temporal inconsistency. Subsequently, video-diffusion-based methods [3, 34, 40] alleviate the problem of temporal inconsistency, relying on the capabilities of the backbone model. However, since U-Net lags behind the DiT architecture [5, 18], these models still face significant challenges in maintaining character identity. Additionally, the lack of text input in existing methods prevents us from further controlling the generated content.

3. Methods

In this work, we present DynamiCtrl in Fig. 2, a new generation paradigm for human image animation that explores pose control within the MM-DiT architecture and re-emphasizes the role of text, diverging from U-Net-based models that require an additional trained pose encoder and discard textual guidance.

3.1. DynamiCtrl Framework

We aim to generate an animated video that maintains identity consistency with a human reference image I while achieving natural movement with a driving video $I_{1:F}$. The driving video frames are the pose sequences which are estimated from the raw motion video. Following a typical

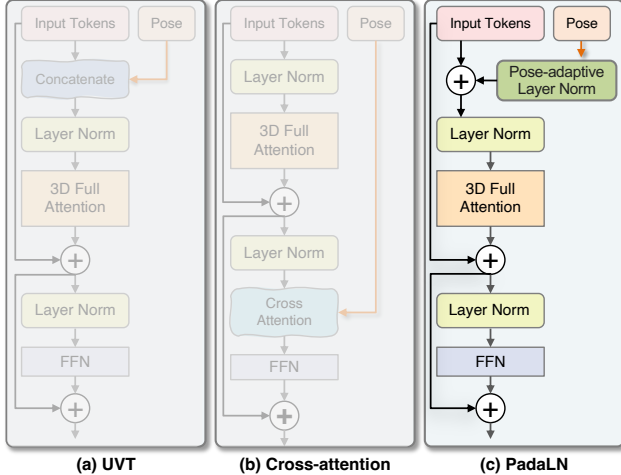


Figure 3. Different pose-guided control structures in MM-DiT.

image-to-video structure [37, 43], we use a VAE encoder \mathcal{E} to extract features \mathcal{F}_i of the human image. We concatenate the \mathcal{F}_i with the noise latent \mathcal{N} as the vision latent. Before entering the MM-DiT block, we need to consider how to extract features from the pose video $I_{1:F}$ and how to incorporate them into the MM-DiT.

Shared VAE Encoder. For pose driving video $I_{1:F} = \{I_1, I_2, \dots, I_F\}$, almost all the previous methods [11, 23, 28, 40] need to train an extra pose encoder to encode the pose video. For instance, Animate Anyone [11] and MimicMotion [40] use shallow convolution layers as the pose guider to encode the pose input, and they initialize the module with Gaussian weights. Disco [28] and MagicAnimate [34] adopt structures like ControlNet [38] to introduce the pose information into the diffusion process. The newly added pose encoder not only increases the complexity of the model architecture, but also brings more training burdens, especially with a design structure like ControlNet [38].

In our design, considering that the MM-DiT block will directly process the visual features after unified encoding, we attempt to use a shared VAE encoder to process both the reference image and the driving video simultaneously. The raw driving video (for $f \times 3 \times h \times w$ frames) is permuted to $3 \times f \times h \times w$ and handled by VAE encoder $\mathcal{E}(I_{1:F})$ to $\mathcal{F}_v \in \mathbb{R}^{F \times C \times H \times W}$. The \mathcal{F}_v is also multiplied by the scaling factor κ of the VAE. During training, the VAE encoder is shared among three signals: the training video, the reference image, and the driving video. This design eliminates the need for additional pose encoders or pose guiders commonly used in traditional models, thereby simplifying the architecture and avoiding extra training. Furthermore, it ensures that the features of these different inputs are aligned in the same embedding space, making it more suitable for the MM-DiT model that requires a unified input of visual tokens. Besides, although MimicMotion [40] mentions that

the training data domain of the VAE encoder is different from that of the pose sequence, our approach shows that using such shared encoding in MM-DiT is still effective.

Bringing Pose Control into MM-DiT After the shared VAE encoder, we get the features \mathcal{F}_v of driving video. To inject the feature into MM-DiT blocks with reference image features \mathcal{F}_i and noise latent \mathcal{N} , we explore three variants of model structures that process pose features differently, shown in Fig. 3. Below, we introduce the details.

- **Unify Vision Token (UVT).** In the I2V backbone, the image features \mathcal{F}_i are concatenated with latent \mathcal{N} with zero padding. The output channel after the VAE encoder is C , so the channel number becomes $2 \times C$. The most straightforward way is to continue concatenating the pose features with these vision tokens, shown in Fig. 3 (a), treating \mathcal{F}_v no differently than the \mathcal{F}_i and the \mathcal{N} . In this way, the channel numbers of latent changes to $2 \times C + C$. In MM-DiT blocks, the unified vision tokens are all used as the query (Q), key (K), and value (V) in full attention. However, an excessively long token sequence will cause the attention mechanism to focus more on local information, leading to instability in long-term learning. Besides, due to the increased channels, we can not load the pre-trained parameters of patch embedding layers.
- **Cross Attention.** In previous video generation works [5, 8, 14, 43], the Cross-Attention (CA) is a widely used structure to fuse the text or image signals with vision features. Following the same design, we try to inject \mathcal{F}_v using cross-attention, shown in Fig. 3 (b). Using feature patchy, we translate feature \mathcal{F}_v to hidden representation $y^g \in \mathbb{R}^{B \times T \times D}$. After 3D full attention, we get the output $\hat{y}^g \in \mathbb{R}^{B \times T \times D}$ of \mathcal{F}_i and \mathcal{N} . In cross-attention, we represents the query (Q), key (K), and value (V) as follows:

$$[Q, K, V] = [W^Q \hat{y}^g, W^K y^g, W^V y^g] \quad (1)$$

After the cross-attention layer, we add the \hat{y}^g and the output together. Under this design, we observe that the effectiveness of pose control is not satisfied, as shown in Fig. 7. The model fails to effectively capture the nonlinear relationship between pose sequences and generated video results, leading to a lack of clear control. Besides, unfortunately, it also introduces a significant increase in parameters, adding up to 40% more.

- **Pose-adaptive Layer Norm (PadaLN).** Before the MM-DiT, DiT framework [18] employs adaptive layer normalization to incorporate data labels into the Transformer for generation. Building on the same concept, we propose the Pose-adaptive Layer Norm (PadaLN), which also utilizes layer norm to integrate pose features \mathcal{F}_v into MM-DiT while preserving the model’s spatiotemporal relationship modeling capacity, shown in Fig. 3 (c). After getting the

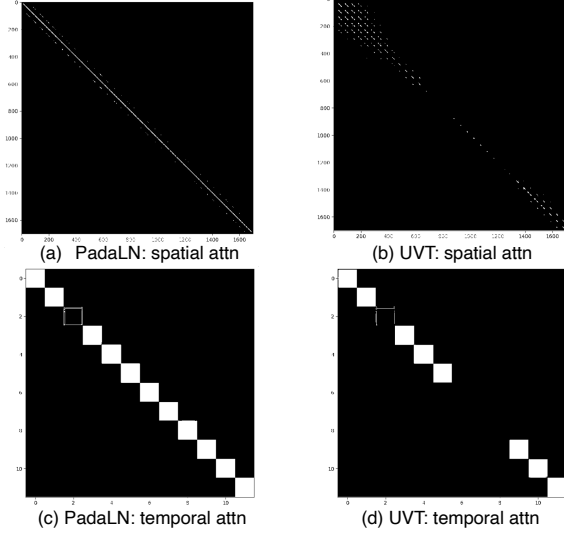


Figure 4. Vision-to-vision spatial and temporal attention visualizations of different control methods.

hidden representation y^g of \mathcal{F}_v , leveraging the MLP, we learn the scale parameter β , shift parameter γ , and gate parameter δ from the embedding vectors of time t :

$$\gamma, \beta, \delta = MLP(SiLU(t)) \quad (2)$$

Before the full attention, we use β and γ to rescale the representation y^g as follows:

$$y_{o1}^g = LN(y^g) * (1 + \beta) + \gamma, \quad (3)$$

where LN denotes the normalization layer. We directly add the y_{o1}^g to the hidden representation of the noise latent. We do not adopt the concatenation method because the element-wise summation operation preserves channel dimensions, thus keeping the model structure unchanged. Besides, before the PadaLN module, we repeat the pose features along the channel dimension to keep the dimensions consistent. The scaled feature y_{o1}^g is calculated by δ to get the input y_{o2}^g for next MM-DiT block, as following:

$$y_{o2}^g = y_{o1}^g + \delta \times y_{o1}^g \quad (4)$$

Among these structures, our ablations in Table 3 show that the PadaLN in DynamiCtrl achieves the best performance. Furthermore, because MM-DiT flattens spatial and temporal tokens for full attention, we visualize the attention maps of MM-DiT with UVT and PadaLN in Fig. 4, showing spatial attention at the single-frame level and temporal attention by tracking tokens at identical spatial positions across different frames. Notably, in MM-DiT with PadaLN, we observe a **distinctive diagonal pattern** for both spatial and temporal attention. The diagonal pattern not only indicates a clear correlation between the spatial position of each frame and its time-related spatial position but also suggests

that each frame in the video has a close temporal dependency with adjacent frames. However, in the UVT, the diagonal pattern is **severely missing in certain regions**. The partial missing of the diagonal portion represents that the model fails to capture the relationships between frames, especially for long-term sequences.

3.2. Refocusing on the Role of Text

In previous works [11, 23, 34, 40], textual information is typically omitted in this task. For instance, Animate Anyone [11] replaces the text input with image features from ReferenceNet, and MimicMotion [40] selects Stable Video Diffusion [2] as the backbone, which also does not contain text input. In this work, we refocus on the role of text and bring it back to the diffusion process for better performance.

Formally, we define the conditions to be a tuple $\mathcal{G} = \langle I, I_{1:F}, \mathcal{C} \rangle$, where \mathcal{C} denotes the space of textual descriptions. We obtain the text feature c from text encoder $Emb(\mathcal{C})$. After processing the input I and driving video $I_{1:F}$ through the VAE encoder \mathcal{E} and PadaLN models, they are added as a unified visual input \mathcal{F}_{vis} and, along with the text tokens c , fed into the MM-DiT. Intuitively, the video generator ρ synthesizes K -step video trajectories that illustrate possible diffusion processes for completing the human animation task with $\{c, \mathcal{F}_{vis}\}$. In the reverse diffusion process, we aim to restore the video using a denoising network ϵ_θ . The prediction paradigm is:

$$\epsilon_\theta(x_t, t, \rho) = \epsilon_\theta(x_t, t, c, \mathcal{F}_{vis}) \quad (5)$$

The whole reverse diffusion process to generate videos with $\{c, \mathcal{F}_{vis}\}$ can be represented as:

$$x_{t-1} = \frac{1}{\sqrt{\alpha_t}} \left(x_t - \frac{1 - \alpha_t}{\sqrt{1 - \alpha_t}} \epsilon_\theta(x_t, t, c, \mathcal{F}_{vis}) \right) + \sigma_t z, \quad (6)$$

$z \sim \mathcal{N}(0, \mathbf{I})$ is the standard Gaussian noise and σ_t is the standard deviation related to timestep t . The whole loss for training with text input of our model is designed as:

$$L = \mathbb{E}_{x_0, t, \epsilon} \left[\|\epsilon - \epsilon_\theta(x_t, t, c, \mathcal{F}_{vis})\|^2 \right], \quad (7)$$

where the ϵ is the added noise. So, we establish the connection between visual and textual signals, enabling the model to be simultaneously guided by human images, driving videos, and prompts. In the ablation presented in Fig. 8 (b), we observe that the textual prompt helps stabilize the generation process and guides the model to achieve higher quality results, which is unachievable in previous works. To further enhance the impact of textual guidance, we incorporate the mask \mathcal{M} of the human image into the training. The \mathcal{F}_{vis} contains only the foreground portrait and its corresponding control pose, while the background is entirely generated and controlled by the text. This training strategy

Methods	Frame Quality					Video Quality	
	L1 (E-04) ↓	SSIM ↑	PSNR ↑	PSNR* ↑	LPIPS ↓	FID-VID ↓	FVD ↓
MagicAnimate [34]	3.13 / 8.21	0.714 / 0.351	29.16 / 21.13	- / 11.44	0.239 / 0.513	21.75 / 85.61	179.07 / 1058.37
Animate Anyone [11]	- / 3.46	0.718 / 0.572	29.56 / 26.60	- / 16.65	0.285 / 0.283	- / 39.26	171.90 / 723.93
Champ [44]	2.94 / 4.23	0.802 / 52.39	29.91 / 25.91	- / 15.78	0.231 / 0.319	21.07 / 25.48	160.82 / 535.96
Unianimate [30]	2.66 / 4.46	0.811 / 0.503	30.77 / 24.34	20.58 / 14.61	0.231 / 0.344	- / 33.39	148.06 / 837.93
MimicMotion [40]	5.85 / 3.60	0.601 / 0.618	- / 27.39	14.44 / 17.09	0.414 / 0.248	- / 23.04	232.95 / 417.56
ControlNext [19]	6.20 / 3.53	0.615 / 0.577	- / 27.89	13.83 / 17.20	0.416 / 0.263	- / 21.16	326.57 / 414.22
StableAnimator [24]	2.87 / 7.86	0.801 / 0.448	30.81 / 23.11	20.66 / 12.00	0.232 / 0.423	- / 22.87	140.62 / 365.46
Animate-X [23]	2.70 / 3.38	0.806 / 0.619	30.78 / 27.42	20.77 / 17.80	0.232 / 0.259	- / 26.95	139.01 / 570.98
DynamiCtrl (Ours)	2.34 / 3.09	0.766 / 0.623	30.22 / 29.43	20.41 / 18.37	0.166 / 0.235	13.77 / 17.15	152.31 / 249.80

Table 2. Quantitative comparisons with SOTAs on TikTok and Unseen100. “PSNR*” [30] denotes the modified metric to prevent numerical overflow. In the table, “a / b”, a, and b denote results on TikTok and Unseen100, respectively. “-” means the missing values in their papers.

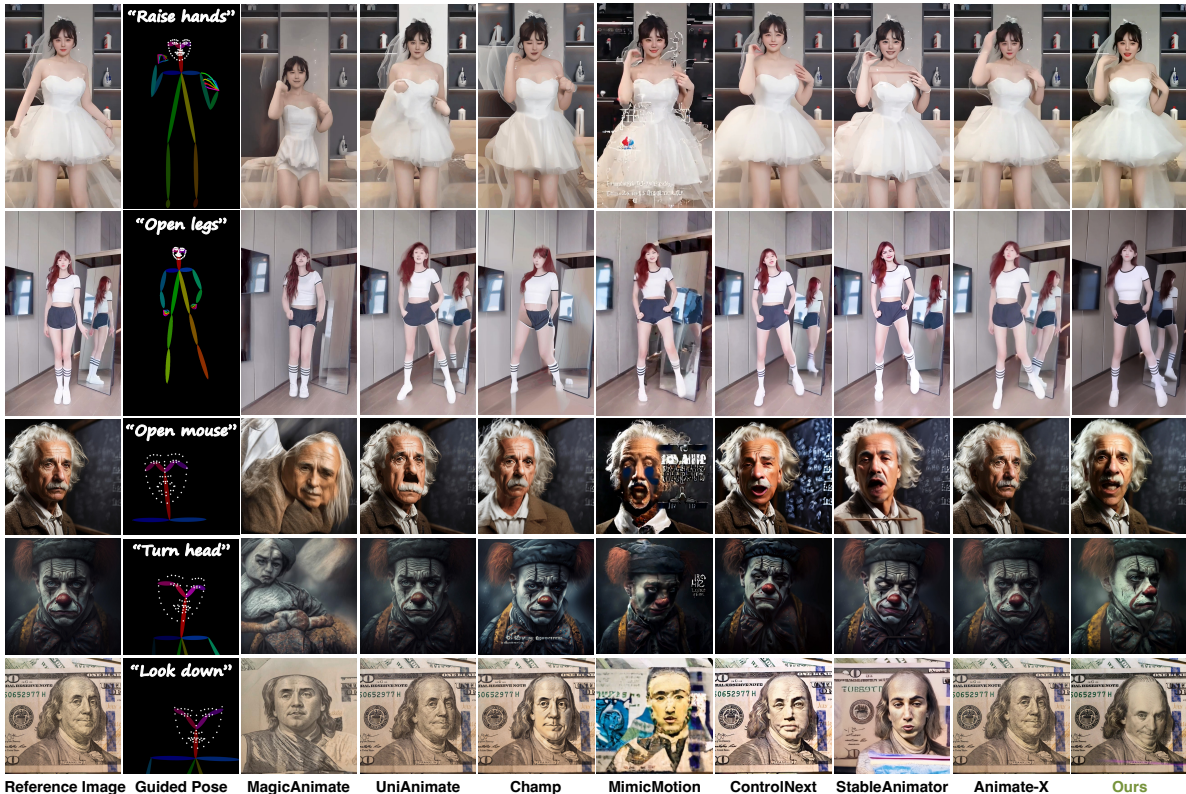


Figure 5. Qualitative comparisons with SOTAs on five challenging unseen examples. We use their released models for generation, and Animate-X [23] is the latest open-source animation model.

allows for flexible background control during inference, as demonstrated in Fig. 6. In particular, by using a long-video inference approach, we achieve innovative scenarios with temporally coherent background transitions and continuous human motion, as illustrated in Fig. 6 (c).

4. Experiments

4.1. Implementation Details

In the proposed DynamiCtrl, we use the DWPose tool [36] to estimate human pose, including body and hand parts. We employ the Qwen2-VL method [27] to obtain image de-

scriptions during both training and inference. To get the mask area of subject in videos, we use the Segment-and-Tracking tool [6]. To evaluate our method, following previous works [3, 11, 24, 28, 40, 44], we use the popular TikTok benchmark [12], which contains 350 videos. We train our method on the training set (1-334) and test on the test set (335-340). Additionally, since the training data of open-source models in previous methods are all private due to human privacy policies, we collect about 13k human motion videos from the internet for training and 100 unseen videos, referred to as Unseen100, as the test set to conduct zero-shot inference. **Evaluation metrics.** Following [23, 28, 34], we



Figure 6. DynamiCtrl can take you anywhere and enable any motion. We provide three examples to demonstrate this capability: (a) Direct background control; (b) Placing the character in different scenes; (c) Long video generation: over 200 frames, showcasing the character moving across seven different scenes while maintaining continuous motion.

adopt the L1, SSIM [31], PSNR [10], LPIPS [39], FID-VID [1] and FVD [25] metrics for evaluation. Besides, the temporal consistency and text alignment based on feature similarity are also conducted for ablation.

4.2. Comparison with State-of-the-Art Methods

Quantitative results. In Table 2, we compare the quantitative results with state-of-the-art methods [19, 23, 24, 30, 40, 44]. We present the test results on the TikTok and Unseen100 datasets. On TikTok, our method achieves the best performance on the L1, LPIPS, and FID-VID metrics, while also delivering comparable results on the PSNR and FVD metrics. Our LPIPS score gets 0.166, representing a 28.1% improvement over the best-performing method [44]. On Unseen100, our method gets the best results across all metrics. To obtain the results of the compared methods, we directly use the open-source codes and models of these models. Due to the challenging cases in the Unseen100, such as complex motions, appearances, and backgrounds, we observe that methods [30, 34] perform worse on this dataset. Notably, since our model is text-controlled, to ensure fairness, we use a text description consistent with the image content during inference, while using the whole human image. Besides, during our experiments, we observe that the FID-VID and FVD metrics do not always exhibit consistent trends. In some test groups, while the FID-VID metric improves, the FVD metric actually worsens.

Qualitative results. In Fig. 5, we provide qualitative comparisons with six state-of-the-art methods [19, 23, 24, 30, 34, 40]. We select five challenging unseen scenes: a person standing in front of a mirror, a girl wearing intri-

cate clothing, the celebrity portrait “Einstein” to assess ID retention, a digitally created made-up person “Joker”, and the abstract human “Franklin” on banknotes, as shown in Fig. 5. We observe that almost all existing methods fail to generate satisfactory results across all reference examples. When both a person and a mirror appear in the scene, existing methods struggle to maintain synchronized motion between the person and their reflection, whereas our approach ensures consistency between the two. In the case of “Einstein”, our method demonstrates a high level of identity preservation and successfully drives the character. Similar results are observed in the examples of the “Joker” and “Franklin”. Although UniAnimate [30] and Animate-X [23] can maintain the identity, they fail to achieve pose-driven animation in these complex cases, making their outputs appear more like direct repetitions of the given reference images. **“Draw” backgrounds with prompts.** By leveraging text, we can achieve more, especially in background control. We provide three cases in Fig. 6. It is observed that we can directly generate any background for the subjects. Notably, in Fig. 6 (c), we show long video results, with over 200 frames. We directly use the last frame of the previous clip as the first frame of the next clip, while changing the background. We successfully maintain temporal consistency and body movement while generating different, dynamic, high-quality backgrounds.

4.3. Ablation Study

The effectiveness of different pose control structures. In our work, we propose three different kinds of pose control structures to introduce the pose sequence into the MM-



Text Prompt: The person in the image is wearing a light gray hoodie with a pattern of small smiley faces. Underneath the hoodie, they are wearing a white crop top with a V-neck design. The person is also wearing a necklace with a cross pendant and a bracelet on their left wrist. The background appears to be an indoor setting, possibly a room, with some shelves and a heart-shaped object visible on the left side.

Text Prompt: The person in the image is wearing a dark blue crop top and black shorts. They are standing on a balcony with a wooden ceiling and a sliding glass door behind them. The background includes a white chair with a cushion, a table, and a view of a building with a balcony. The overall setting appears to be a modern, well-lit space with a serene outdoor view.

Text Prompt: The person in the image is wearing a light gray cardigan over a white blouse with a bow tie. The blouse has a plaid skirt with blue and white stripes. The person has long, dark hair and is wearing glasses. The background appears to be an indoor setting with a white wall and a door or window with a glass panel. There is also a refrigerator visible on the left side of the image.

Figure 7. Ablation of DynamiCtrl with different pose control methods across three examples and PadaLN performs best.

Methods	Image Quality			Video
	SSIM \uparrow	PSNR* \uparrow	LPIPS \downarrow	FVD \downarrow
DynamiCtrl (w/ UVT)	0.613	17.25	0.267	508.25
DynamiCtrl (w/ CA)	0.586	16.20	0.279	518.90
DynamiCtrl (w/ PadaLN)	0.766	20.41	0.166	152.31

Table 3. Effectiveness of different pose control structures.

DiT for human image animation. Here we provide the ablation of different DynamiCtrl models with these control structures on TikTok in Table 3. It can be found that PadaLN achieves the best performance in both image and video qualities. Besides, we also provide the visualization results of these structures in Fig. 7. In UVT, we observe the disappearance of details, blurriness, and visual defects. As shown in Fig 4, we attribute this phenomenon to the method disrupting the temporal consistency of the video. The cross-attention exhibits poor pose control performance. We believe the reason is, when performing cross-attention in the high-dimensional sequence of full attention, it fails to focus on the sparse pose features in the driving video.

Methods	Image Quality			Video
	SSIM \uparrow	PSNR* \uparrow	LPIPS \downarrow	FVD \downarrow
DynamiCtrl (w/o text)	0.723	18.93	0.198	221.10
DynamiCtrl (w/ text)	0.766	20.41	0.166	152.31

Table 4. Effect of Text on Training (with or without).

The effectiveness of text control. Compared with previous works [11, 19, 23, 24, 34, 40], we are the first to investigate the role of textual prompts in this task. In addition

to directly using text to control background generation, we also conduct ablation studies in Table 4 to understand how text influences model training. We conduct training and inference on the TikTok dataset with and without textual prompts. The results show that the model’s performance significantly decreases without text input. Furthermore, we demonstrate how text enhances video quality in Fig. 8. It shows that text can help control character motion with the driving pose and correct visual artifacts, respectively. It is worth noting that previous methods cannot achieve these effects, as they lack fine-grained textual input.

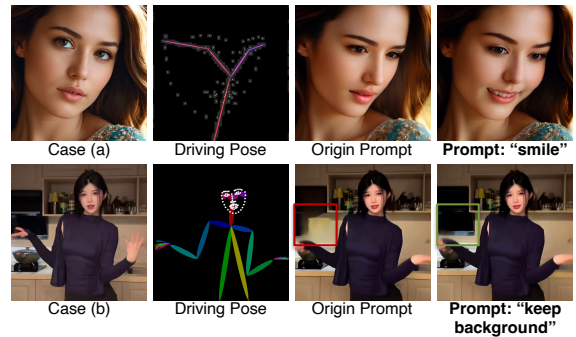
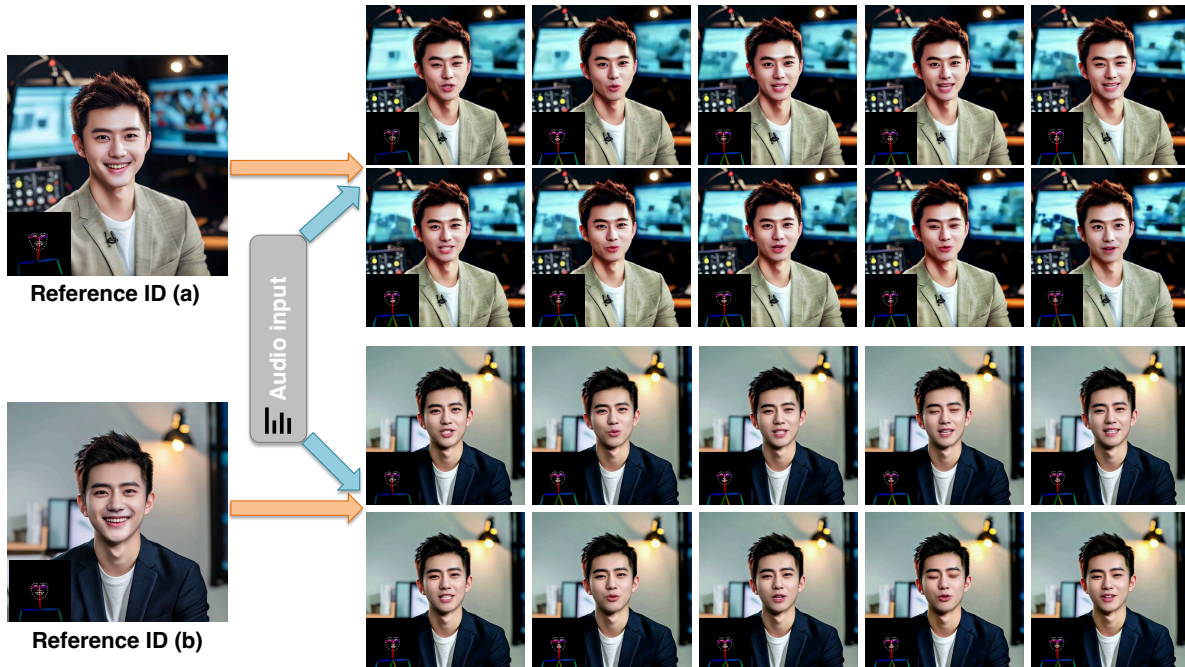


Figure 8. Ablation study on the impact of text on content.

Ablation of aligned image and text. Our model employs both images and text as conditions. We conduct ablations to analyze their respective effects with a full human image. As shown in Fig. 10, we find that the model performs best when the text aligns with the image content. However, when the two are mismatched, the model performs worse.



* Appearance (a) and (b) are generated by vivo BlueLM (text to image model).

Figure 9. Visualization of digital humans. Given the digital human appearances (a) and (b), we can generate vivid digital human representations based on audio content. First, DynamiCtrl is used to generate the video content, including body movements and facial expressions, based on the control pose. Second, the mouth movements are redrawn according to the audio content using the MuseTalk [41] algorithm.

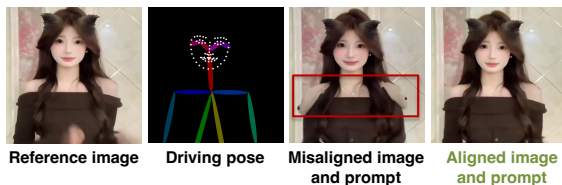


Figure 10. Effectiveness of aligned image and text as inputs.

Methods	Temporal consistency \uparrow	Text alignment \uparrow
Baseline	97.519	26.490
Ours (w/ Group 1)	97.866	27.124
Ours (w/ Group 2)	97.596	27.129
Ours (w/ Group 3)	97.609	26.971

Table 5. Ablation of video quality under different backgrounds.

Ablation of background control with different prompts.

We conduct experiments to evaluate the model’s performance under different textual conditions when controlling background generation on TikTok. The baseline denotes the results without background control. We experiment with different prompts (groups 1-3) to replace the background. The results in Table 5 demonstrate that the DynamiCtrl model maintains strong temporal consistency while ensuring textual alignment.

Methods	ID preservation \uparrow	Motion-align \uparrow	Visual quality \uparrow
MimicMotion [40]	22.22	17.78	15.56
ControlNext [19]	22.22	14.44	18.89
StableAnimator [24]	14.45	21.11	17.78
Animate-X [23]	14.44	22.23	14.44
Ours	26.67	24.44	33.33

Table 6. User study of human preferences with 12 volunteers evaluating 15 unseen data samples.

4.4. User Study and More Applications

In Table 6, we provide the results of the user study from a human visual perception perspective. Additionally, we consider real-world scenarios and their applications, such as digital humans, shown in Fig. 9.

5. Conclusion

In this work, we proposed DynamiCtrl, a novel framework based on MM-DiT for human image animation. Instead of an extra pose encoder, we leveraged the Shared VAE encoder for vision inputs. Our Pose-adaptive Layer Norm effectively injects pose features into attention, enabling precise control. Additionally, we reemphasized the role of text and achieved multi-faceted control, including backgrounds. Extensive experiments confirmed that DynamiCtrl generates high-quality, identity-preserving, heterogeneous character driving, and highly controllable human motion videos.

References

- [1] Yogesh Balaji, Martin Renqiang Min, Bing Bai, Rama Chellappa, and Hans Peter Graf. Conditional gan with discriminative filter generation for text-to-video synthesis. In *IJCAI*, page 2, 2019. 7
- [2] Andreas Blattmann, Tim Dockhorn, Sumith Kulal, Daniel Mendelevitch, Maciej Kilian, Dominik Lorenz, Yam Levi, Zion English, Vikram Voleti, et al. Stable video diffusion: Scaling latent video diffusion models to large datasets. *arXiv preprint arXiv:2311.15127*, 2023. 2, 3, 5
- [3] Di Chang, Yichun Shi, Quankai Gao, Hongyi Xu, Jessica Fu, Guoxian Song, Qing Yan, Yizhe Zhu, Xiao Yang, and Mohammad Soleymani. Magicpose: Realistic human poses and facial expressions retargeting with identity-aware diffusion. In *ICML*, 2023. 2, 3, 6
- [4] Haoxin Chen, Yong Zhang, Xiaodong Cun, Menghan Xia, Xintao Wang, Chao Weng, and Ying Shan. Videocrafter2: Overcoming data limitations for high-quality video diffusion models. In *CVPR*, pages 7310–7320, 2024. 2, 3
- [5] Shoufa Chen, Mengmeng Xu, Jiawei Ren, Yuren Cong, Sen He, Yanping Xie, Animesh Sinha, Ping Luo, Tao Xiang, and Juan-Manuel Perez-Rua. GenTron: Diffusion transformers for image and video generation. In *CVPR*, pages 6441–6451, 2024. 2, 3, 4
- [6] Yangming Cheng, Liulei Li, Yuanyou Xu, Xiaodi Li, Zongxin Yang, Wenguan Wang, and Yi Yang. Segment and track anything. *arXiv preprint arXiv:2305.06558*, 2023. 6
- [7] Patrick Esser, Sumith Kulal, Andreas Blattmann, Rahim Entezari, Jonas Müller, Harry Saini, Yam Levi, Dominik Lorenz, Axel Sauer, Frederic Boesel, et al. Scaling rectified flow transformers for high-resolution image synthesis. In *ICML*, 2024. 2
- [8] Jiaxi Gu, Shicong Wang, Haoyu Zhao, Tianyi Lu, Xing Zhang, Zuxuan Wu, Songcen Xu, Wei Zhang, Yu-Gang Jiang, and Hang Xu. Reuse and diffuse: Iterative denoising for text-to-video generation. *arXiv preprint arXiv:2309.03549*, 2023. 2, 3, 4
- [9] Jonathan Ho, Ajay Jain, and Pieter Abbeel. Denoising diffusion probabilistic models. In *NeurIPS*, 2020. 3
- [10] Alain Hore and Djemel Ziou. Image quality metrics: Psnr vs. ssim. In *ICPR*, pages 2366–2369. IEEE, 2010. 7
- [11] Li Hu. Animate anyone: Consistent and controllable image-to-video synthesis for character animation. In *CVPR*, pages 8153–8163, 2024. 2, 3, 4, 5, 6, 8
- [12] Yasamin Jafarian and Hyun Soo Park. Learning high fidelity depths of dressed humans by watching social media dance videos. In *CVPR*, pages 12753–12762, 2021. 6
- [13] Johanna Karras, Aleksander Holynski, Ting-Chun Wang, and Ira Kemelmacher-Shlizerman. Dreampose: Fashion image-to-video synthesis via stable diffusion. In *ICCV*, pages 22623–22633. IEEE, 2023. 2, 3
- [14] Zhimin Li, Jianwei Zhang, Qin Lin, Jiangfeng Xiong, Yanxin Long, Xinchu Deng, Yingfang Zhang, Xingchao Liu, Minbin Huang, Zedong Xiao, et al. Hunyuan-dit: A powerful multi-resolution diffusion transformer with fine-grained chinese understanding. *arXiv preprint arXiv:2405.08748*, 2024. 2, 3, 4
- [15] Yue Ma, Yingqing He, Xiaodong Cun, Xintao Wang, Siran Chen, Xiu Li, and Qifeng Chen. Follow your pose: Pose-guided text-to-video generation using pose-free videos. In *AAAI*, pages 4117–4125, 2024. 2, 3
- [16] MooreThreads/Moore-AnimateAnyone. May 2024. [Online], original-date: 2024-01-12T07:55:21Z. <https://github.com/MooreThreads/Moore-AnimateAnyone>. 2
- [17] Haomiao Ni, Bernhard Egger, Suhas Lohit, Anoop Cherian, Ye Wang, Toshiaki Koike-Akino, Sharon X. Huang, and Tim K. Marks. Ti2v-zero: Zero-shot image conditioning for text-to-video diffusion models. In *CVPR*, pages 9015–9025. IEEE, 2024. 3
- [18] William Peebles and Saining Xie. Scalable diffusion models with transformers. In *ICCV*, pages 4195–4205, 2023. 2, 3, 4
- [19] Bohao Peng, Jian Wang, Yuechen Zhang, Wenbo Li, Ming-Chang Yang, and Jiaya Jia. Controlnext: Powerful and efficient control for image and video generation. *arXiv preprint arXiv:2408.06070*, 2024. 6, 7, 8, 9
- [20] Bosheng Qin, Wentao Ye, Qifan Yu, Siliang Tang, and Yueting Zhuang. Dancing avatar: Pose and text-guided human motion videos synthesis with image diffusion model. *arXiv preprint arXiv:2308.07749*, 2023. 2, 3
- [21] Robin Rombach, Andreas Blattmann, Dominik Lorenz, Patrick Esser, and Björn Ommer. High-resolution image synthesis with latent diffusion models. In *CVPR*, pages 10684–10695, 2022. 3
- [22] Aliaksandr Siarohin, Oliver J Woodford, Jian Ren, Menglei Chai, and Sergey Tulyakov. Motion representations for articulated animation. In *CVPR*, pages 13653–13662, 2021. 2, 3
- [23] Shuai Tan, Biao Gong, Xiang Wang, Shiwei Zhang, Dandan Zheng, Ruobing Zheng, Kecheng Zheng, Jingdong Chen, and Ming Yang. Animate-x: Universal character image animation with enhanced motion representation. *ICLR*, 2024. 2, 4, 5, 6, 7, 8, 9
- [24] Shuyuan Tu, Zhen Xing, Xintong Han, Zhi-Qi Cheng, Qi Dai, Chong Luo, and Zuxuan Wu. Stableanimator: High-quality identity-preserving human image animation. *arXiv preprint arXiv:2411.17697*, 2024. 2, 6, 7, 8, 9
- [25] Thomas Unterthiner, Sjoerd Van Steenkiste, Karol Kurach, Raphael Marinier, Marcin Michalski, and Sylvain Gelly. Towards accurate generative models of video: A new metric & challenges. *arXiv preprint arXiv:1812.01717*, 2018. 7
- [26] Fanyi Wang, Peng Liu, Haotian Hu, Dan Meng, Jingwen Su, Jinjin Xu, Yanhao Zhang, Xiaoming Ren, and Zhiwang Zhang. Loopanimate: Loopable salient object animation. *arXiv preprint arXiv:2404.09172*, 2024. 2, 3
- [27] Peng Wang, Shuai Bai, Sinan Tan, Shijie Wang, Zhihao Fan, Jinze Bai, Keqin Chen, Xuejing Liu, Jialin Wang, Wenbin Ge, et al. Qwen2-vl: Enhancing vision-language model’s perception of the world at any resolution. *arXiv preprint arXiv:2409.12191*, 2024. 6
- [28] Tan Wang, Linjie Li, Kevin Lin, Yuanhao Zhai, Chung-Ching Lin, Zhengyuan Yang, Hanwang Zhang, Zicheng Liu, and Lijuan Wang. Disco: Disentangled control for realistic human dance generation. In *CVPR*, pages 9326–9336, 2024. 2, 3, 4, 6

- [29] Xiang Wang, Hangjie Yuan, Shiwei Zhang, Dayou Chen, Jiuniu Wang, Yingya Zhang, Yujun Shen, Deli Zhao, and Jingren Zhou. Videocomposer: Compositional video synthesis with motion controllability. *arXiv preprint arXiv:2306.02018*, 2023. 3
- [30] Xiang Wang, Shiwei Zhang, Changxin Gao, Jiayu Wang, Xiaoqiang Zhou, Yingya Zhang, Luxin Yan, and Nong Sang. Unianimate: Taming unified video diffusion models for consistent human image animation. *arXiv preprint arXiv:2406.01188*, 2024. 6, 7
- [31] Zhou Wang, Alan C Bovik, Hamid R Sheikh, and Eero P Simoncelli. Image quality assessment: from error visibility to structural similarity. *TIP*, 13(4):600–612, 2004. 7
- [32] Zhiqiang Xia, Zhaokang Chen, Bin Wu, Chao Li, Kwok-Wai Hung, Chao Zhan, Yingjie Hu, and Wenjiang Zhou. Musev: Infinite-length and high fidelity virtual human video generation with visual conditioned parallel denoising, 2024. <https://github.com/TMElyralab/MuseV>. 2, 3
- [33] Jiaqi Xu, Xinyi Zou, Kunzhe Huang, Yunkuo Chen, Bo Liu, MengLi Cheng, Xing Shi, and Jun Huang. Easyanimate: A high-performance long video generation method based on transformer architecture. *arXiv preprint arXiv:2405.18991*, 2024. 2, 3
- [34] Zhongcong Xu, Jianfeng Zhang, Jun Hao Liew, Hanshu Yan, Jia-Wei Liu, Chenxu Zhang, Jiashi Feng, and Mike Zheng Shou. Magicanimate: Temporally consistent human image animation using diffusion model. In *CVPR*, pages 1481–1490, 2024. 3, 4, 5, 6, 7, 8
- [35] Ceyuan Yang, Zhe Wang, Xinge Zhu, Chen Huang, Jianping Shi, and Dahua Lin. Pose guided human video generation. In *ECCV*, pages 201–216, 2018. 2
- [36] Zhendong Yang, Ailing Zeng, Chun Yuan, and Yu Li. Effective whole-body pose estimation with two-stages distillation. In *ICCV*, pages 4210–4220, 2023. 6
- [37] Zhuoyi Yang, Jiayan Teng, Wendi Zheng, Ming Ding, Shiyu Huang, Jiazheng Xu, Yuanming Yang, Wenyi Hong, Xiaohan Zhang, Guanyu Feng, et al. Cogvideox: Text-to-video diffusion models with an expert transformer. *arXiv preprint arXiv:2408.06072*, 2024. 2, 3, 4
- [38] Lvmin Zhang, Anyi Rao, and Maneesh Agrawala. Adding conditional control to text-to-image diffusion models. In *ICCV*, pages 3813–3824. IEEE, 2023. 4
- [39] Richard Zhang, Phillip Isola, Alexei A Efros, Eli Shechtman, and Oliver Wang. The unreasonable effectiveness of deep features as a perceptual metric. In *CVPR*, pages 586–595, 2018. 7
- [40] Yuang Zhang, Jiayi Gu, Li-Wen Wang, Han Wang, Junqi Cheng, Yuefeng Zhu, and Fangyuan Zou. Mimicmotion: High-quality human motion video generation with confidence-aware pose guidance. *arXiv preprint arXiv:2406.19680*, 2024. 2, 3, 4, 5, 6, 7, 8, 9
- [41] Yue Zhang, Minhao Liu, Zhaokang Chen, Bin Wu, Yubin Zeng, Chao Zhan, Yingjie He, Junxin Huang, and Wenjiang Zhou. Musetalk: Real-time high quality lip synchronization with latent space inpainting. *arXiv preprint arXiv:2410.10122*, 2024. 9
- [42] Zihao Zhang, Haoran Chen, Haoyu Zhao, Guansong Lu, Yanwei Fu, Hang Xu, and Zuxuan Wu. Eden: Enhanced diffusion for high-quality large-motion video frame interpolation. *CVPR*, 2025. 3
- [43] Haoyu Zhao, Tianyi Lu, Jiayi Gu, Xing Zhang, Qingping Zheng, Zuxuan Wu, Hang Xu, and Yu-Gang Jiang. Magdiff: Multi-alignment diffusion for high-fidelity video generation and editing. In *ECCV*, pages 205–221. Springer, 2025. 2, 3, 4
- [44] Shenhao Zhu, Junming Leo Chen, Zuozhuo Dai, Zilong Dong, Yinghui Xu, Xun Cao, Yao Yao, Hao Zhu, and Siyu Zhu. Champ: Controllable and consistent human image animation with 3d parametric guidance. In *ECCV*, pages 145–162. Springer, 2024. 2, 6, 7